Paper

Modelling of the Temperature and Current Dependence of LED Spectra

Frank REIFEGERSTE and Jens LIENIG

TU Dresden, Institute of Electromechanical and Electronic Design, www.ifte.de

Received March 4, 2008, Accepted May 20, 2008

ABSTRACT

Spectra of LED devices show a noticeable temperature and current dependence. Often this behaviour can be neglected. However, some applications like spectrometry or narrow band imaging take advantage of the spectral characteristics of LEDs. In such cases knowledge about the spectral behaviour is relevant. This article describes a measurement setup for investigating the influence of temperature and current on the spectral radiation of LED. Results from measurements are presented. Appropriate mathematical functions for modelling LED spectra are discussed and their applicability is rated. A new formalism for modelling of LED spectra in consideration of current and temperature is derived. With this approach, the prediction accuracy of the spectral behaviour is increased significantly.

KEYWORDS: LED, light emitting diodes, spectral analysis, temperature, current, modelling

1. Introduction

LED devices have developed rapidly over the last years with an average improvement of flux per package of 20x per decade[1]. This has lead to an enormous improvement of the luminous efficacy and output power per device. Thus, LED devices have become attractive for new applications, not only for signage but also for illumination. For general illumination the small spectral bandwidth is rather unfavourable and leads to the development of techniques for spectral broadening like stimulation of phosphors. However, other applications like machine vision profit from this nearly monochromatic spectrum, for example by using spectrally optimised lenses. Another usage of LED illuminations is for spectroscopic applications like narrow band imaging which also takes advantage of the narrow spectral characteristic. The spectral behaviour of LEDs for these applications cannot be neglected. The dependence of the spectrum on operating conditions and on environment ought to be known. This paper describes research done to describe and model this dependence.

2. Background

The spectra of recent LED devices depend on operating current or voltage and on temperature. This dependence is often not precisely characterised in the device data sheets. Not all manufacturers specify the spectral behaviour. Often, only the parameter dominant wavelength λ_d is used for characterisation. It is not possible to derive the shape of the radiation spectrum from the data sheet information. To specify the spectral behaviour, further measurements are necessary.

By using a spectrometer, it is easily possible to measure the spectral radiometric output of a source. However, cost considerations often forbid the integration of a spectrometer in the light source for practical purposes. If the dependences of LED spectra on environmental conditions are to be considered, the appropriate modelling of those dependences is possible.

For this purpose it would be desirable to derive the spectral characteristics strictly from a physical device model. The generation-recombination equilibrium depends on two processes: the carrier distribution of the allowed states in the semiconductor and the density of states in the semiconductor[2]. The output spectrum of an LED is then controlled by the two terms temperature T and magnitude of the bandgap E_g of the semiconductor. Equation (1) depicts this proportionality.

$$I(E) \propto \sqrt{E-E_g} \cdot e^{-\frac{E}{k \cdot T}} \quad (1)$$

Theoretically, the spectral behaviour shown in Figure 1 is expected. In accordance with this theoretical prediction, measurements show that the spectral characteristic depends significantly on the junction temperature and the operating voltage of the diode[3)4)]. However, actual devices have a different characteristic which cannot be explained with this first order model. An example is shown in Figure 2.

The different behaviour of the real LED compared to the theoretical expectation results from a number of additional semiconductor effects that contribute extra terms to Eq.(1). Normally, a user is not able to survey all these contributions because they depend on unstated semiconductor properties. This problematic motivates the search for functions which are suitable to describe the spectral characteristic phenomenologically. Nevertheless, it is desirable that the parameters used in the model function can be interpreted directly. For instance, it should be possible to derive the peak emission wavelength λ_p directly from the equation. Additionally, models should be composed such that they can be easily used in practical applications. Free parameters should have values which can be easily measured. Since LEDs are mostly driven by current sources in technical application, the operating current and not the LED voltage is considered as a variable in this paper.

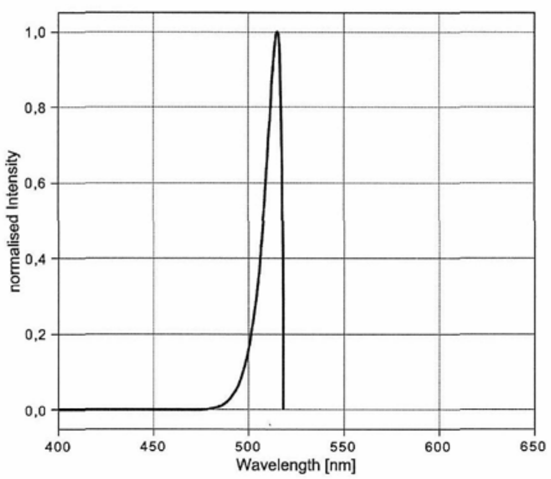

Figure 1 Theoretic spectrum of an LED with E_g=2.4eV and ϑ_j=33.7°C[2]

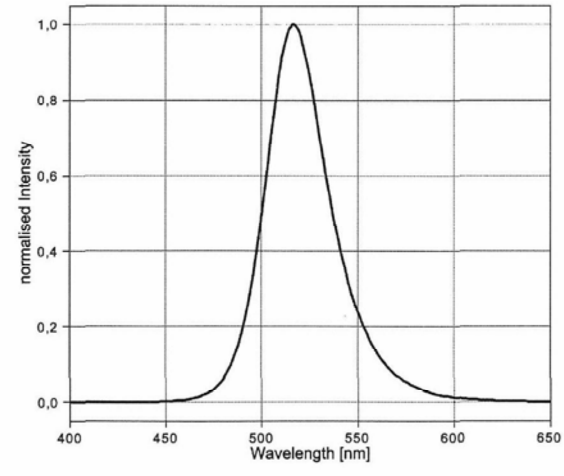

Figure 2 Measured spectrum of an LED HLMP-CM31-M00DD at i_{LED}=20mA and ϑ_j=33.7°C

3. Measurement

3.1 Measurement setup

In order to explore the dependence of real LEDs on temperature and operating current, the radiated spectrum is measured under defined currents and temperatures. For this purpose, a measurement setup as shown in Figure 3 is chosen. The device under test is thus located within a solid block with a constant temperature.

Current i_{LED} is driven by a precision current source with different current values of 1mA, 2mA, 5mA, 10mA and 20mA. The setup is placed within a temperature controlled lab. The device under test is mounted within a drill-hole inside a copper block which is heated by four resistive heaters. The diode and particularly its cathode are flange mounted thermally in respect to this block. Furthermore, a Pt100 temperature sensor is mounted within the assembly near the diode. Measurement and control of temperature are done by a commercial available temperature controller (Omron E5CN-C2MT-500 24VAC/DC). A proportional control scheme is used. An absolute accuracy of better than 1K and a setpoint stability of <0.2 K are maintained. Temperatures from 20°C to 100°C with steps of 20K are used for measurement.

It is known that the diode voltage and the operating current cause a thermal power loss inside the LED. This in turn increases the temperature of the LED and should therefore be considered. The contributions from convection and radiation can be neglected, because the LED is completely surrounded by the heating block except for the light exit and the temperature difference in respect of the surrounding is small. Thus only the resulting heat flux must be modelled. The ambience can be assumed to be a thermal ground of constant temperature since the LED is connected thermally to the temperature regulated block. For calculations, a maximum power dissipation of 60 mW and a maximum operating current of 20 mA are assumed.

To estimate the temperature gradient inside the LED, a finite element method (FEM) simulation was done using the modelling system Comsol Femlab 3.2. By modelling the setup specified above, the temperature gradient shown in Figure 4 was calculated. The excess

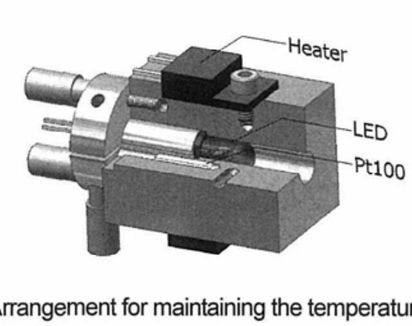

Figure 3 Arrangement for maintaining the temperature of LED

temperature of the LED chip is 13.7 K. This corresponds to a thermal resistance of R_{th}=228 K/W for this setup. In the literature, thermal resistance values of R_{th}=(210-260) K/W[5)6)], R_{th}=(200-300) K/W[7)] and R_{th}=240 K/W[8)] are reported. Considering the good thermal coupling of the diode in this setup, the calculated value seems plausible to the authors.

In the above model, only thermal conduction is considered. The thermal conductivity of the utilised materials in the range of 0-120°C is nearly constant. Hence, a simplified thermoelectric equivalent circuit, depicted in Figure 5, is used for calculating the actual chip temperature.

The excess temperature in respect to thermal ground can be calculated by Equation (2).

$$\Delta T_{ja} = R_{th} \cdot P_v \quad (2)$$

For commonly used values of current i_{LED}, the results shown in Table 1 are obtained.

The accuracy of simulation can be increased by calculating the actual chip power dissipation from the values of i_{LED} and u_{LED} and subtracting the optical output power. All spectra were measured with a spectrometer type Zeiss MMS1. For each LED, 25 different spectra (five currents, each at five temperature values) are measured. As devices under test different LEDs from leading manufacturers with various semiconductor materials shown in Table 2 are chosen. All units have a T1 3/4 (5 mm) plastic housing to be comparable.

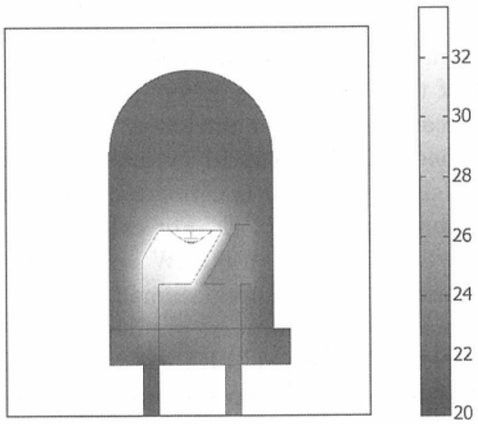

Figure 4 Temperature distribution inside a 5 mm LED at 60 mW loss power in°C

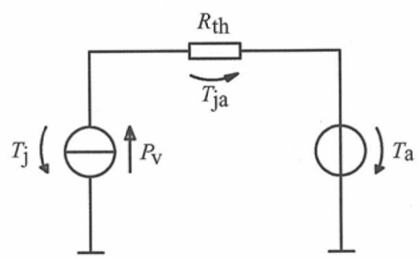

Figure 5 Equivalent circuit for calculating the chip temperature

3.2 Measurement results

The measurements described above were taken for several LEDs. Due to space limitations, not all results can be shown here. Figures 6 and 7 depict exemplary investigated spectra in standardised representation at different operating conditions. It can be seen that the sample in Figure 6 shows a noticeable dependence of the peak wavelength on temperature while the sample in Figure 7 shows a noticeable current dependence of the peak wavelength.

Table 1 Temperature difference between junction and ambient for different currents

Current i_{LED} [mA]	Temperature difference ΔT_{ja} [K]
1	0.7
2	1.4
5	3.4
10	6.9
20	13.7

Table 2 Considered LED types

Manufacturer	LED type	Semiconductor material	Peak wavelength λ_p [nm] from data sheet
Avago Technologies	HLMP-CE30-N0000	InGaN	502
Avago Technologies	HLMP-CM31-M00DD	InGaN	524
Nichia Corporation	NSPG510S	InGaN	525
Stanley Electric Co.	EBG5304S	GaP	555
Vishay Semiconductors	TLCPG5102-DD2	AlInGaP/GaAs	563

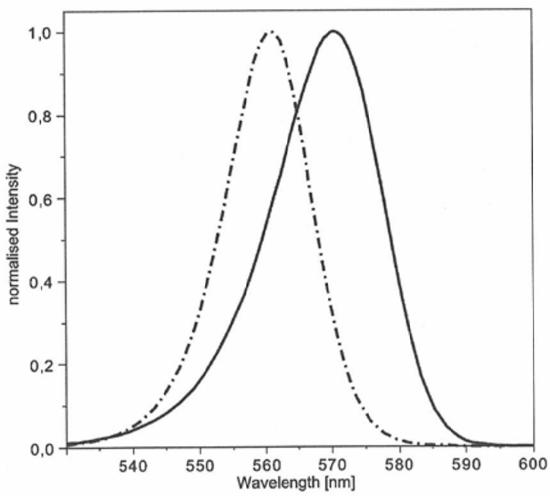

Figure 6 Spectra of an LED TLCPG5100-DD2 at ϑ_j=33.7°C (dashed line) and at ϑ_j=113.7°C (solid line), respectively, and i_{LED}=20 mA operating current in normalised representation

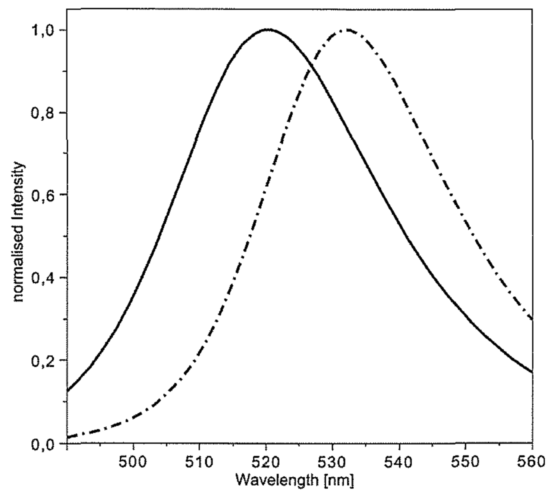

Figure 7 Spectra of an LED HLMP-CM31-M00DD at i_{LED}=1 mA and ϑ_j=20.7°C (dashed line) and at i_{LED}=20 mA and ϑ_j=33.7°C (solid line) in normalised representation

4. Modelling

4.1 Model functions

Mathematically based models should be investigated to approximate LED spectra phenomenologically because no physical model has been reported which approximates LED spectra sufficiently. Since real spectra are mostly non-symmetrical this behaviour ought to be considered. Models from the literature[3)9)] should be compared to the found models. Possible functions should meet several requirements, such as:

- have a shape and parameterisation that is appropriate,
- approximate measured spectral values with good accuracy,
- be evaluated easily,
- possess parameters which can be interpreted directly (e.g. peak wavelength),
- possess parameters which can be obtained easily from spectral measurement.

The functions shown in Table 3 were examined.

Equations (3) and (6) are symmetric and therefore inappropriate for the mostly asymmetric spectra. We list them nevertheless because of their multiple usage in literature. Equation (12) approximates spectra very well but the parameters cannot be interpreted directly. The function is defined piecewise. An extension of this model for varying temperatures and currents is not possible. Therefore it is not suitable here. With this in mind, Equation (5) is not easy to formalise either. One possibility to consider the asymmetry is to split the equation into two ranges – one to the left of the maximum and one to the right as done in Equations (4) and (10). Also here the mathematical formalism is cumbersome for optimization because the functions are not uniformly continuous. In Equation (11), two skew parameters are used and the parameters cannot be interpreted directly. The remaining Equations (7), (8) and (11) are eligible for modelling LED spectra. Parameters A and C can be interpreted directly as intensity and peak wavelength respectively for these equations.

Table 3 Examined approximation functions

Function name	Function $f(\lambda)$	
Gaussian[3)]	$f(\lambda)=A\cdot e^{-\left(\frac{\lambda-C}{W}\right)^2}$	(3)
Split Gaussian	$f(\lambda)=A\cdot e^{-\left(\frac{\lambda-C}{W}\right)^2}$ with $W=W_1$ for $\lambda<C$, $W=W_2$ otherwise	(4)
Sum of Gaussians	$f(\lambda)=A_1\cdot e^{-\left(\frac{\lambda-C_1}{W_1}\right)^2}+A_2\cdot e^{-\left(\frac{\lambda-C_2}{W_2}\right)^2}$	(5)
Second order Lorentzian[5)]	$f(\lambda)=\frac{A}{\left(1+\left(\frac{\lambda-C}{W}\right)^2\right)^2}$	(6)
Logistic power peak	$f(\lambda)=\frac{A}{S}\left(1+e^{\frac{\lambda-C+W\cdot\ln(S)}{W}}\right)^{\frac{-S-1}{S}}\cdot e^{\frac{\lambda-C+W\cdot\ln(S)}{W}}\cdot(S+1)^{\frac{S+1}{S}}$	(7)
Asymmetric logistic peak	$f(\lambda)=A\cdot\left(1+e^{-\frac{\lambda-C+W\cdot\ln(S)}{S}}\right)^{-S-1}\cdot S^{-S}\cdot(S+1)^{S+1}\cdot e^{-\frac{\lambda-C+W\cdot\ln(S)}{W}}$	(8)
Pearson VII	$f(\lambda)=\frac{A}{\left(1+\left(\frac{\lambda-C}{W}\right)^2\cdot\left(2^{\frac{1}{S}}-1\right)\right)^S}$	(9)
Split Pearson VII	$f(\lambda)=\frac{A}{\left(1+\left(\frac{\lambda-C}{W}\right)^2\cdot\left(2^{\frac{1}{S}}-1\right)\right)^S}$ with $W=W_1$, $S=S_1$ for $\lambda<C$ and $W=W_2$, $S=S_2$ otherwise	(10)
Asymmetric Double sigmoidal	$f(\lambda)=\frac{A}{1+e^{-\frac{\lambda-C+\frac{W}{2}}{S_1}}}\cdot\left(1-\frac{1}{1+e^{-\frac{\lambda-C+\frac{W}{2}}{S_2}}}\right)$	(11)
Piecewise 3rd order polynomial (spline)	piecewise: $f(\lambda)=a_3x^3+a_2x^2+a_1x+a_0$ piecewise definition for n ranges $x_{k-1}\le x<x_k$, $k=1..n$	(12)

4.2 Model evaluation

The stated requirement of simple calculation of the fitting parameters mentioned in the previous chapter cannot be satisfactorily fulfilled. Parameter computation is non-trivial for some of these functions as they are non-linear and cannot be linearised by common methods. For this reason, methods of non-linear optimization such as programs Maple™ 11 with Global Optimization Toolbox and fityk 0.8.3 are used. Due to this methodology, the results are not analytically optimal. However, the findings show that the results are stable and reproducible. The relative 'least squares R-value' *SSR* was calculated for the evaluation of the fitting quality between fit and measurement data. Smaller values represent a better fit. The results of the investigation for an LED type HLMP-CM31-M00DD are depicted in Table 4. Values written in brackets cannot be interpreted directly. They are shown only for reference.

Table 4 Parameter findings for Equations (3), (6), (7), (8), (9) and (11) for an LED HLMP-CM31-M00DD at i_{LED}=20 mA and ϑ_j=33.7°C

Equation	Parameter				Relative SSR
	A	C	W	S	
Eq. (3)	3217.0	524.54	(21.59)	NA	0.392
Eq. (6)	3622.6	522.48	(28.29)	NA	$71.95 \cdot 10^{-3}$
Eq. (7)	3556.5	520.27	(8.33)	(2.02)	$4.21 \cdot 10^{-3}$
Eq. (8)	3482.6	520.37	(13.75)	(2.97)	$2.97 \cdot 10^{-3}$
Eq. (9)	3490.0	522.57	(19.25)	(3.72)	$62.93 \cdot 10^{-3}$
Eq. (11)	(12674.2)	(514.94)	(3.00)	(S_1=7.51), (S_2=15.59)	$2.15 \cdot 10^{-3}$

Multiple experiments with different LEDs and different semiconductor systems show that Equation (7) is most suitable for approximating LED spectra, hence it is subsequently used. Table 5 displays parameter findings for Equation (7) for a number of LEDs driven with a constant current of i_{LED}=20 mA and a junction temperature of ϑ_j =33.7°C. The parameters A and C can be interpreted directly in this equation.

4.3 Model extension

The model described above allows the approximation of the spectral behaviour of an LED at one operating point defined by the operating current i_{LED} and the junction temperature ϑ_j. It would be desirable to expand the model for arbitrary operating currents and junction temperatures. Here it must be regarded that the spectral characteristic depends on the operating current and junction temperature. However the junction temperature itself also depends on the loss power.

To model this behaviour, parameters A, C, W and S of Equation (7) were calculated for each current-temperature setpoint. Table 6 shows determined values of parameters A, C, W and S for the different current-temperature combinations of one device. It is obvious that these parameters can be modelled as functions of operating current i_{LED} and junction temperature ϑ_j. Equations (13) to (16) are suitable for modelling of the associated parameters A, C, W and S.

$$A(T,i) = a_0 \cdot T^{a_T} \cdot i^{a_i} \qquad (13)$$

$$C(T,i) = c_0 + c_T \cdot T + c_i \cdot \log(i) \qquad (14)$$

$$S(T,i) = s_0 + s_T \cdot T + s_i \cdot \log(i) \qquad (15)$$

$$W(T,i) = w_0 + w_T \cdot T + w_i \cdot i \qquad (16)$$

Parameters [a_0, a_T, a_i] in Equation (13), [c_0, c_T, c_i] in Equation (14), [s_0, s_T, s_i] in Equation (15) and [w_0, w_T, w_i] in Equation (16) can be calculated by using methods of non-linear optimization. For the example shown in Table 6, parameter values shown in Table 7 can be derived.

Utilizing Equations (13) to (16), it is now possible to predict the parameters A, C, S and W for arbitrary i_{LED} / ϑ_j setpoints. Figures 8 and 9 depict the position of the peak wavelength in dependence on the operating current i_{LED} and the junction temperature ϑ_j calculated from Equation (14) as an example.

By substituting each parameter of Equation (7) with its associated Equations (13) to (16), Equation (17) is obtained, which only depends on the operating current i_{LED} and the junction temperature ϑ_j. Hence, it is possible to predict the characteristic of the emitted spectrum at an arbitrary current-temperature setpoint.

$$f(T,i,\lambda) = \frac{A(T,i)}{S(T,i)} \left[1 + e^{\frac{\lambda - C(T,i) + W(T,i) \cdot \ln(S(T,i))}{W(T,i)}} \right]^{\frac{-S(T,i)-1}{S(T,i)}} \cdot e^{\frac{\lambda - C(T,i) + W(T,i) \cdot \ln(S(T,i))}{W(T,i)}} \cdot \left[S(T,i) + 1 \right]^{\frac{S(T,i)+1}{S(T,i)}} \qquad (17)$$

Table 5 Parameter findings for Equation (7) for different LEDs at i_{LED}=20 mA and ϑ_j=33.7°C

Manufacturer	LED type	A	C	W	S	Relative SSR
Avago Technologies	HLMP-CE30-N0000	3261.9	500.5	6.90	2.19	$1.23 \cdot 10^{-3}$
Avago Technologies	HLMP-CM31-M00DD	3556.5	520.3	8.33	2.02	$4.21 \cdot 10^{-3}$
Nichia	NSPG510S	3682.3	521.4	7.07	2.27	$1.37 \cdot 10^{-3}$
Stanley	EBG5304S	1971.5	555.5	5.65	1.68	$9.15 \cdot 10^{-3}$
Vishay	TLCPG5102-DD2	2833.9	560.9	5.00	0.53	$5.05 \cdot 10^{-3}$

Table 6 Parameter findings for Equation (7) for an LED HLMP-CM31-M00DD at different i_{LED} and ϑ_j

LED operating current i_{LED}									
1 mA		2 mA		5 mA		10 mA		20 mA	
ϑ_j [°C]	Parameter	ϑ_j [°C]	Parameter	ϑ_j [°C]	Parameter	ϑ_j [°C]	Parameter	ϑ_j [°C]	Parameter
20.7	A=267.5 C=532.1 W=7.23 S=2.22	21.4	A=531.5 C=529.7 W=7.37 S=2.20	23.4	A=1211.5 C=526.5 W=7.71 S=2.14	26.9	A=2127.0 C=523.7 W=8.04 S=2.06	33.7	A=3556.5 C=520.3 W=8.33 S=2.02
40.7	A=245.5 C=532.7 W=7.56 S=2.12	41.4	A=492.1 C=530.2 W=7.64 S=2.12	43.4	A=1133.9 C=526.9 W=8.00 S=2.05	46.9	A=2000.8 C=524.1 W=8.41 S=1.97	53.7	A=3354.7 C=521.1 W=8.86 S=1.88
60.7	A=223.1 C=533.3 W=7.97 S=2.00	61.4	A=450.6 C=530.9 W=8.03 S=2.01	63.4	A=1048.1 C=527.5 W=8.40 S=1.94	66.9	A=1860.3 C=524.8 W=8.82 S=1.86	73.7	A=3130.7 C=521.9 W=9.37 S=1.76
80.7	A=202.1 C=534.1 W=8.42 S=1.89	81.4	A=411.9 C=531.8 W=8.52 S=1.88	83.4	A=968.5 C=528.4 W=8.84 S=1.83	86.9	A=1732.1 C=525.7 W=9.30 S=1.75	93.7	A=2949.7 C=522.9 W=9.92 S=1.64
100.7	A=187.8 C=534.9 W=8.92 S=2.22	101.4	A=388.1 C=532.7 W=9.05 S=2.20	103.4	A=930.4 C=529.5 W=9.35 S=2.14	106.9	A=1729.2 C=526.8 W=9.83 S=2.06	113.7	A=3311.4 C=524.1 W=10.48 S=2.02

Table 7 Parameter findings for Equations (13) to (16) for the values from Table 6

Equation	Parameter value		
Eq.(13)	a_0=161221.5	a_T=0.845	a_i=-0.137
Eq.(14)	c_0=504.1	c_T=$0.391 \cdot 10^{-1}$	c_i=-3.946
Eq.(15)	s_0=1.964	s_T=$-0.553 \cdot 10^{-2}$	s_i=$-0.569 \cdot 10^{-1}$
Eq.(16)	w_0=6.670	w_T=0.225	w_i=55.47

Figures 10 and 11 demonstrate this predictability by comparing two modelled spectra at (i_{LED}=10 mA, ϑ_j=76.8°C) and (i_{LED}=20mA, ϑ_j=104.7°C) with measured spectra at these setpoints. Both pictures indicate that the model function approximates the real behaviour at any setpoint within the considered range. The relative *SSR* value for these cases is $3.31 \cdot 10^{-3}$ and $1.57 \cdot 10^{-3}$, respectively.

5. Conclusions

In this paper, investigations have been described to determine functions which are appropriate for modelling the spectrum of real light emitting diodes. It has been shown that the "Logistic power peak" function is most suitable for modelling the spectral behaviour. The parameters of this function are simple to comprehend.

Additionally, spectral dependences of these parameters on the physically well measurable quantities current and temperature were investigated. It has been shown that it is possible to fit simple functions to these dependences. Combined with an appropriate spectral modelling function, a new model has been developed which predicts the spectrum of an LED only from operating current i_{LED} and the junction temperature ϑ_j. By this means it is possible to calculate the spectral behaviour of a previously investigated LED. Thus, the accuracy of the spectral prediction is increased significantly.

Model parameters must be determined for each LED. This effort is only justified if the spectral response from

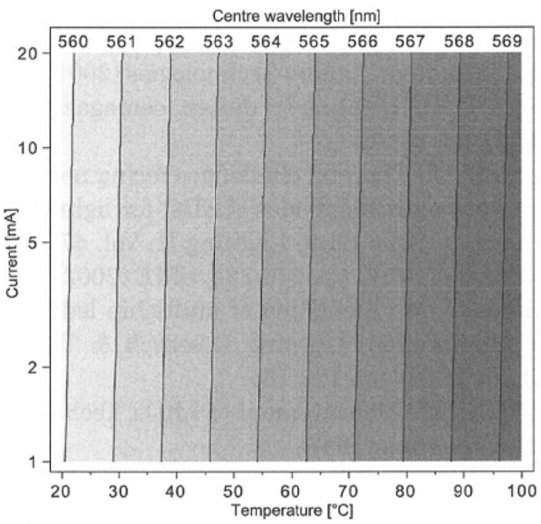

Figure 8 Current-temperature dependence of the peak wavelength of an LED TLCPG5100-DD2

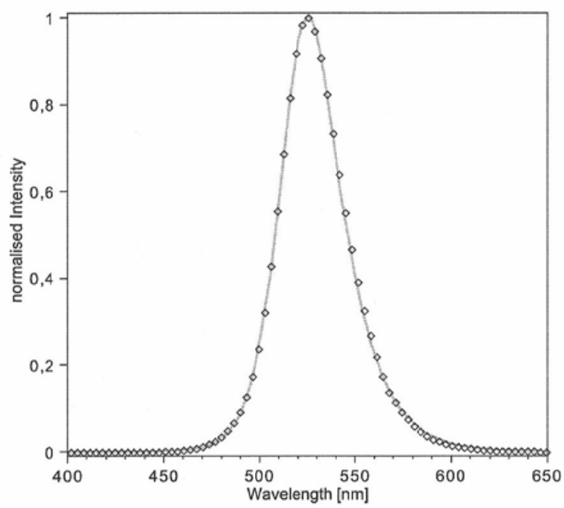

Figure 10 Comparison of a modelled spectrum at i_{LED}=10mA and ϑ_j=76.8°C (solid line) and the measured dataset at this setpoint (squares)

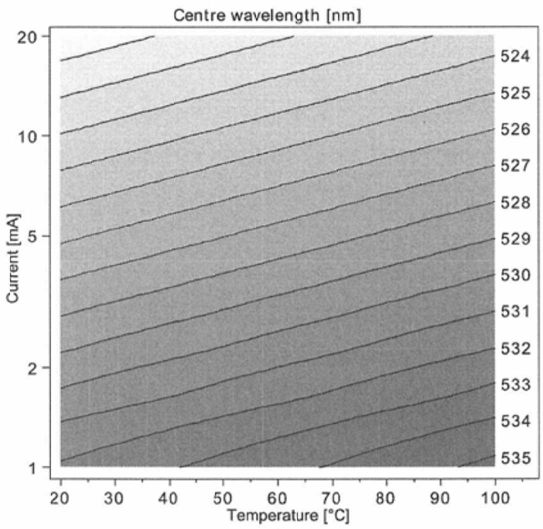

Figure 9 Current-temperature dependence of the peak wavelength of an LED HLMP-CM31-M00DD

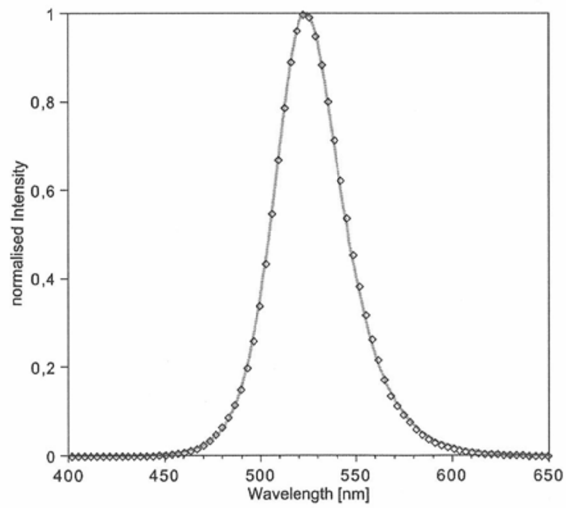

Figure 11 The same curve pattern at a different setpoint (i_{LED}=20 mA, ϑ_j=104.7°C) indicates the precise approximation of the experimental data by Equation (17)

an LED cannot be measured during operation but rather should be known precisely. Further work will investigate how the parameters depend on the lifetime of LED.

Symbols and nomenclature

<Symbol>		<Explanation>
A	…	Modelling parameter 'amplitude'
C	…	Modelling parameter 'centre'(equals to λ_p for most functions)
E_g	…	Energy of semiconductor bandgap
$HWHM$	…	Half width half maximum
i_{LED}	…	LED operating current
λ	…	Wavelength
λ_d	…	Dominant wavelength, for definition see[10)]
λ_p	…	Peak wavelength
P_v	…	Loss power
R_{th}	…	Thermal resistance of LED case
S	…	Modelling parameter 'skew'
SSR	…	Least sum of squared residuals
T	…	Temperature
ΔT_{ja}	…	Temperature difference between junction and ambient
ϑ_j	…	Junction temperature
u_{LED}	…	LED voltage
W	…	Modelling parameter 'width'

References

(1) Haitz, R.: Advances in Solid State Physics, chap. Another Semiconductor revolution: This Time It's Lighting!, pp. 35-50, Springer, Berlin (2003).

(2) Schubert, F. E.: Light-Emitting Diodes, Cambridge University Press, Cambridge, 1st edn. (2003).

(3) Chhajed, S., Xi, Y., Gessmann, T., Xi, J.-Q., Shah, J. M., Kim, J. K. and Schubert, E. F.: Junction temperature in light-emitting diodes assessed by different methods, in Light-Emitting Diodes: Research, Manufacturing, and Applications IX, Vol. 5739 of Proceedings of SPIE, pp. 16-24, SPIE (2005).

(4) Hong, E. and Nadendran, N.: A method for projecting useful life of led lighting systems, in Third international conference on solid state lighting, Vol. 5187 of Proceedings of SPIE, pp. 93-99, SPIE (2003).

(5) Thermal resistance values for led lamps — application brief i-002, Tech. Rep., Agilent Technologies (1999).

(6) Led lamp thermal properties — application brief a04, Tech. Rep., Agilent Technologies (2001).

(7) Pelka, D. G.: Lighting by design, oemagazine, SPIE, (2005): pp. 26-28.

(8) Petroski, J.: Thermal challenges facing new generation light emitting diodes (LEDs) for lighting applications, in Solid State Lighting II, Vol. 4776 of Proceedings of SPIE, pp. 215-222, SPIE (2002).

(9) Gaines, J. M.: Modelling of multichip led packages for illumination, Lighting Research & Technology, Vol. 38 (2006): pp. 153-165.

(10) CIE, Cie127: Measurement of LEDs, Tech. Rep. CIE 127, CIE, Wien (1997).